Fundamental Research xxx (xxxx) xxx

Contents lists available at ScienceDirect

Fundamental Research

journal homepage: http://www.keaipublishing.com/en/journals/fundamental-research/

Review

Emergent quantum phenomena in atomically engineered iridate heterostructures

Lin Hao[a], Di Yi[b], Meng Wang[c], Jian Liu[d,*], Pu Yu[e,f,*]

[a] Anhui Key Laboratory of Condensed Matter Physics at Extreme Conditions, High Magnetic Field Laboratory, HFIPS, Chinese Academy of Sciences, Hefei, Anhui 230031, China
[b] State Key Lab of New Ceramics and Fine Processing, School of Materials Science and Engineering, Tsinghua University, Beijing 100084, China
[c] RIKEN Center for Emergent Matter Science (CEMS), Wako 351-198, Japan
[d] Department of Physics and Astronomy, University of Tennessee, Knoxville, Tennessee 37996, USA
[e] State Key Laboratory of Low Dimensional Quantum Physics and Department of Physics, Tsinghua University, Beijing 100084, China
[f] Frontier Science Center for Quantum Information, Beijing 100084, China

ARTICLE INFO

Article history:
Received 28 May 2022
Received in revised form 22 September 2022
Accepted 25 September 2022
Available online xxx

Keywords:
Iridate
Spin-orbit coupling
Many-body physics
Artificial crystalline structure
Magnetism
Magnetotransport property
Ionic liquid gating

ABSTRACT

Over the last few years, researches in iridates have developed into an exciting field with the discovery of numerous emergent phenomena, interesting physics, and intriguing functionalities. Among the studies, iridate-based artificial structures play a crucial role owing to their extreme flexibility and tunability in lattice symmetry, chemical composition, and crystal dimensionality. In this article, we present an overview of the recent progress regarding iridate-based artificial structures. We first explicitly introduce several essential concepts in iridates. Then, we illustrate important findings on representative $SrIrO_3$/$SrTiO_3$ superlattices, heterostructures comprised of $SrIrO_3$ and magnetic oxides, and their response to external electric-field stimuli. Finally, we comment on existing problems and promising future directions in this exciting field.

1. Introduction

Due to the strong spin-orbit coupling (SOC), compounds containing 5*d* elements have gained increasing attention with the emergence of enormous exciting findings. Among the extensive collection of materials, iridates are particularly notable for being a rare playground that covers plenty of foremost research topics, such as frustrated magnetism, topological phases of matter, and superconductivity [1–8]. Pioneering works include those hunting for exotic magnetic states in complex lattice compounds, such as the hyper-kagome iridate $Na_4Ir_3O_7$ [9]. The search of the quantum spin liquid state is expanded to iridates with a honeycomb lattice unit, e.g., Na_2IrO_3 and Li_2IrO_3, for possible implementation of the exotic Kiteav physics in t_{2g} compounds [10–12]. In the early stage, Na_2IrO_3 also attracted attention from the topological physics community, and it was proposed that the honeycomb iridate could be effectively described with the same Hamiltonian [13] as the one used for graphene. The latter is notable for the realization of the quantum hall effect [14]. Another celebrated thread to realize topological nontrivial phases was launched through the theoretical studies of the pyrochlore iridate family $A_2Ir_2O_7$, where *A* is yttrium or a lanthanide element. It was suggested that the compound could be a topological Mott insulator [15,16] or a Weyl semimetal [17], depending on the delicate balance among lattice distortion, electron correlation, magnetic structure, etc.

Early outstanding works in the iridates community also include the exotic electronic structure of Sr_2IrO_4, which should be a half-filled nonmagnetic metal in the band picture [18] but turns out to be a good magnetic insulator [19]. It was suggested that the insulating nature is driven by the collective interactions among strong SOC, crystal-field splitting, and electron correlation, because of which this compound is dubbed as a spin-orbit Mott insulator [18]. In contrast to the rather complicated lattice structure of honeycomb or pyrochlore iridates, Sr_2IrO_4 features a much simpler lattice structure, where square lattices composing of corner-sharing IrO_6 octahedra stack alternately with rock-salt SrO layers. The close analogy in lattice structure between Sr_2IrO_4 and the par-

* Corresponding authors: Tsinghua University, State Key Laboratory of Low Dimensional Quantum Physics and Department of Physics, Beijing 100084, China; University of Tennessee, Department of Physics and Astronomy, Knoxville, Tennessee 37996, USA.
E-mail addresses: jianliu@utk.edu (J. Liu), yupu@mail.tsinghua.edu.cn (P. Yu).

https://doi.org/10.1016/j.fmre.2022.09.030

Please cite this article as: L. Hao, D. Yi, M. Wang et al., Emergent quantum phenomena in atomically engineered iridate heterostructures, Fundamental Research, https://doi.org/10.1016/j.fmre.2022.09.030

ent phase of high-T_C cuprates, La_2CuO_4, naturally raises a question on whether the former is a candidate material for pursuing superconductivity. Indeed, later theoretical works demonstrated that the compound is a promising platform to realize the half-filled single-orbital spin-1/2 Hubbard model [20]. The potential routes to achieve iridate-based superconductivity eventually boost the research of iridates into a hot stage [20,21]. Similar to the 2D-limit Sr_2IrO_4, $SrIrO_3$ is another key member of the Ruddlesden-Popper series for the strontium iridates, but in the 3D limit, where an IrO_6 octahedron shares corners with six nearest neighbors, forming a perovskite lattice structure. Theoretically, a bunch of nontrivial topological phases were proposed even in this simple perovskite iridate, through certain lattice engineering or external stimuli [22,23]. Later experimental work indeed demonstrated that while the perovskite $SrIrO_3$ is a paramagnetic semimetal as expected due to its enhanced dimensionality, the metallicity, in fact, has a more intriguing nature [24,25].

Works mentioned above highlight the exotic nature of the emergent phenomena unveiled from bulk compounds of iridates, which have been nicely summarized in several early elegant reviews [1–8,26]. These reviews cover some specific topics, such as topological properties of complex iridates [1], square-lattice iridates [6], and iridates of the 5+ valence state [8]. In complementary to these bulk-sample researches, a large amount of effort has been invested in integrating iridates with other transition-metal oxides to build up artificial structures, which are unobtainable through conventional bulk synthesis. The most commonly adopted building block is the perovskite $SrIrO_3$, which is mainly due to its structural analogy with many prototype transition metal oxides (e.g., manganites, ruthenates) and the availability of appropriate single-crystal substrates. Thanks to the rapid development of advanced growth techniques with atomic precision, this field grows rapidly and frequently delivers emerging phenomena beyond bulk compounds and other oxide heterostructures. In this review, we aim to provide a brief (by no means exhaustive) overview of recent exciting findings in iridate-based artificial structures, which is not or only partially covered in previous reviews [27–31]. We will first briefly introduce several basic concepts in iridates in Section 2, serving as the ABCs for readers to step into this exciting field. In Section 3, we discuss emergent phenomena associated with the energetic charge and spin fluctuations in quasi-2D $J_{\rm eff} = 1/2$ square lattice built from artificial structures with *about-isolated* iridates. In Section 4, we review works on anomalous/topological Hall effects and magnetic anisotropy in artificial structures with magnetically coupled iridates and various magnetic oxides. Section 5 focuses on emergent electronic states in the iridate-based artificial structures through ionic evolution. Finally, we present our future perspectives on this exciting field in Section 6.

2. Basic concepts of iridates

The fascinatingly rich phase diagram of iridates is usually ascribed to the intriguing interplay of several essential physical parameters, such as on-site electron-electron correlation (the Hubbard interaction U), crystal-field splitting, and on-site SOC, and we note that all these are comparable at the similar energy scale. It thus would be instructive to show how the SOC shifts the conventional paradigm from the perspectives of both the atomic- and the many-body- levels. In traditional 3d transition metal compounds, SOC is typically tiny and can be treated as a perturbation. The orbital momentum $\boldsymbol{L}$ and the electron spin momentum $\boldsymbol{S}$ are thus decoupled, leading to the $|l_z,\ s_z\rangle$ Hilbert space, which is a direct product of orbital space and spin space. Interestingly, the crystalline 5d orbital features an effective $\boldsymbol{L}_{\rm eff} = -1$, rather than =2, because the sizeable cubic field effect splits the atomic d orbital into three t_{2g} orbitals and two e_g orbitals [18], while the latter is far higher in energy and can be integrated out safely in most cases [10]. The fact that projection of the $\boldsymbol{L}$ operator for the d electrons on the t_{2g} orbitals (yz, xz, xy) have an opposite matrix representation of the $\boldsymbol{L}$ operator in the basis of p orbitals (p_x, p_y, p_z), gives rise to the extra negative sign [8]. Subject to the spin-conservation restriction, inter-site electron hopping in this basis is always real and spin-independent.

The eigenstates are changed drastically when SOC is sufficiently strong to entangle the $|l_z,\ s_z\rangle$ states, in which one has to adopt a new representation defined by $|J_{\rm eff},\ m_{J_{eff}}\rangle$. Here, the effective total angular momentum $\boldsymbol{J_{eff}}$ is the addition of effective orbital momentum $\boldsymbol{L}_{\rm eff}$ and $\boldsymbol{S}$. More explicitly, the strong SOC hybridizes the effective orbital space with spin space, giving rise to a half-filled $J_{\rm eff} = 1/2$ doublet and $J_{\rm eff} = 3/2$ quartet. Notably, the latter $J_{\rm eff} = 3/2$ quartet is lower in energy and fully occupied by four d electrons in iridates, as shown in Fig. 1a [32]. Thus, the most relevant states are the $J_{\rm eff} = 1/2$ Kramers doublet, which can be described as a pseudospin one-half due to a peculiar spin density distribution and quasi-isotropic charge density in the real space under an equal mixture of t_{2g} orbitals, as schematically shown in Fig. 1b [10]. The central idea of the new wavefunctions is that the electron hopping between neighboring sites can be pseudospin dependent and complex, which is the key for realizing nontrivial topological phases of matter [13]. Schematically shown in Fig. 1c is a representative electron hopping process leading to a pseudospin-dependent integral in the presence of octahedral rotation and tilting. One may note that the uniform $J_{\rm eff} = 1/2$ state can only be realized in an ideal cubic crystal field, while octahedral distortions, like tetragonal distortion by stretching or compressing along the diagonal direction, are mostly inevitable in a realistic material [10]. Nevertheless, later works show that the $J_{\rm eff} = 1/2$ picture is usually a good starting point for studying iridates, while subtle modulation, including octahedral distortions, cross hopping through the excited $J_{\rm eff} = 3/2$ state, etc. further enriches the electronic states.

3. Energetic charge and spin fluctuations

Over the past decades, intense researches on layered iridates have reached a consensus that the 2D pseudospin square lattice is of great importance in many-body physics and inspired one to further manipulate this 2D unit. Representative works along this direction include the one made by Matsuno et al., who designed and fabricated several superlattice (SL) structures composed of perovskite $SrIrO_3$ and $SrTiO_3$ monolayers, aiming to produce artificial-crystal analogies to the bulk compounds [33]. The obtained [$(SrIrO_3)n/(SrTiO_3)1$] SLs display a metal-to-insulator transition as a function of the $SrIrO_3$ layer number (n), indeed similar to the Ruddlesden-Popper iridate series. More interestingly, a nonzero spontaneous magnetization emerges in stark contrast to the about-zero magnetization in the bulk counterparts. Later then, Hao et al. expanded the SL family [$(SrIrO_3)n/(SrTiO_3)m$] to include the freedom of the $SrTiO_3$ (insulating spacer) thickness further to modulate the interlayer magnetic coupling [34]. While all the SLs remain a spin-orbit Mott insulator, the authors found interesting changes in the magnetic properties with varying m. The critical role of the $SrTiO_3$ block firstly manifests on the antiferromagnetic (AFM) ordering temperature T_N, which decreases dramatically when m increases from 1 to 2 in [$(SrIrO_3)1/(SrTiO_3)m$], suggesting a significantly suppressed interlayer coupling. However, T_N is almost unchanged from $m = 2$ to $m = 3$, although the latter is supposed to have a weaker interlayer coupling than the former SL. This observation sets a strong evidence that the [$(SrIrO_3)1/(SrTiO_3)m$] SLs with $m \geq 2$ is in the 2D limit, where the interlayer magnetic coupling is no longer dominant in determining T_N.

In addition to the intriguing change in the coupling magnitude, sign modulation of the interlayer coupling was also established. As schematically shown in Fig. 2a, the interlayer coupling is positive/negative if m is odd/even. Furthermore, the sign switching of interlayer coupling is always conjugated with the modulation of octahedral rotation patterns, leading to the alignment of spin-canting induced net magnetic moments in each $SrIrO_3$ layer and thus a nonzero spontaneous magnetization in the whole SL series. The enriched diversity in terms of lattice structure and physical properties of the [$(SrIrO_3)n/(SrTiO_3)m$] SLs renders them as a fertile platform to host various research topics, as introduced below.

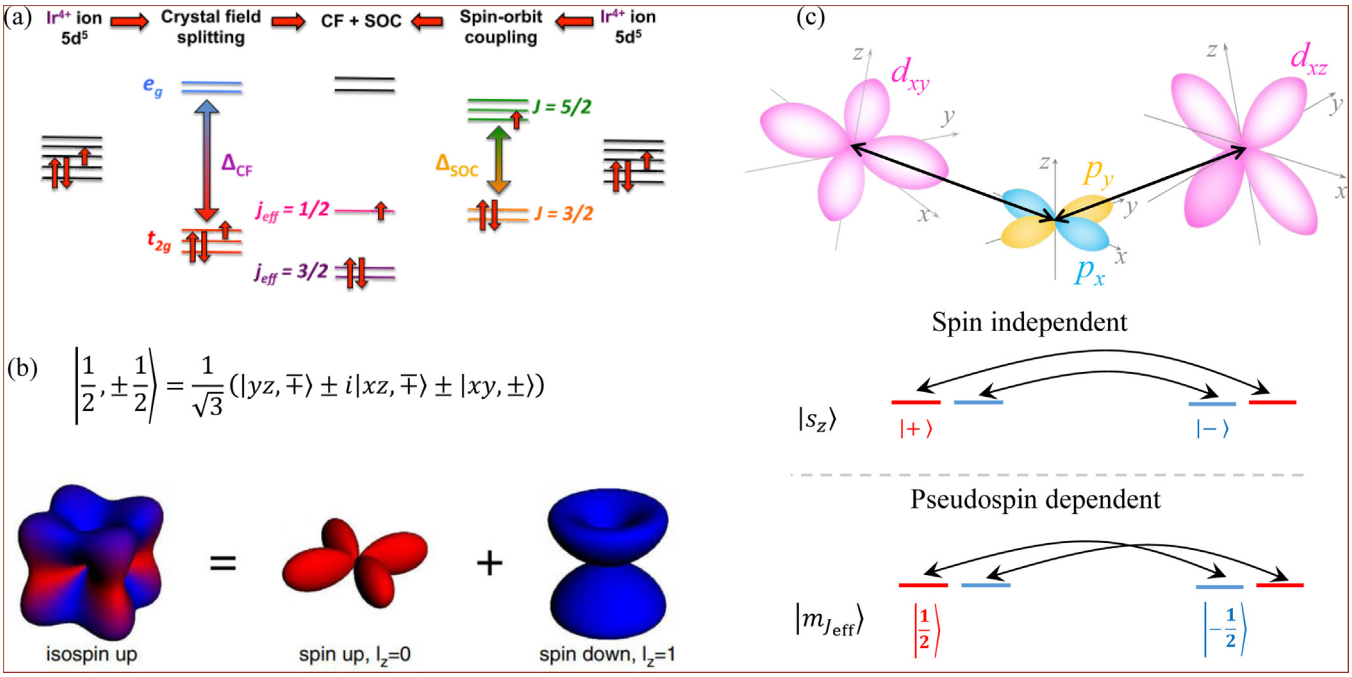

Fig. 1. Basic concepts of iridates. (a) 5*d*-orbital level splitting due to the cubic crystal field and strong SOC. (b) Density profile of a $J_{\text{eff}} = 1/2$ pseudospin (isospin up) state. (c) A representative inter-site electron hopping mediated by oxygen ligands. Local inversion symmetry breaking leads to pseudospin dependent hopping as schematically shown in the bottom panel. Panel (a) adapted from Ref. [27]. Panel (b) adapted from Ref. [10].

One of the most puzzling observations in earlier layered iridates studies (including those of artificial structures) is the presence of a resistivity anomaly around the AFM transition [33,35]. While this feature was typically ascribed to an inter-coupling between electronic property and magnetic order, a closer inspection is necessary to achieve a deeper understanding. Hao et al. then carried out a case study on the $[(SrIrO_3)1/(SrTiO_3)1]$ SL [36], considering the simplicity of its lattice and magnetic structures. In this case, one can view the SL as a simple stack of equally separated pseudospin square lattice with identical magnetic and lattice structures. The resistivity anomaly of the SL is in fact a sharp upturn of resistivity when cooling through T_{N}. After applying an in-plane magnetic field, the resistivity increases dramatically around T_{N} and this upturn is gradually smeared. The extracted magnetoresistance (MR) effect is positive and displays a diverging-like behavior, similar to the magnetic susceptibility, as shown in Fig. 2b.

The energetic charge response indicates that substantial charge fluctuations exist even above T_{N}, and couple with AFM fluctuations to respond to the external magnetic field. To cope with this intriguing picture, an effective 2D half-filled Hubbard model was employed based on the fact that the SL is dominated by a half-filled $J_{\text{eff}} = 1/2$ band around the Fermi level [33]. The theoretical analysis unveils that while the insulating ground state is expected at zero temperature independent of electron correlation, spin-charge fluctuations above T_{N} is the strongest in the case with moderate electron correlation. Explicitly speaking, while the electron correlation can support an insulating state above T_{N}, it is far from the strong limit to completely freeze the charge degree of freedom. Therefore, the charge fluctuations strongly entangle with longitudinal spin fluctuations, as evidenced by the large positive in-plane MR. Upon suppressing the spin fluctuations with a magnetic field by virtue of staggered field effect, the density of effective charge carriers is reduced, giving rise to the anomalous MR effect that characterizes the spin longitudinal susceptibility (Fig. 2c). It is clear that the effective carrier-density driven MR effect is fundamentally different from conventional MR effects that usually originates from the change of carrier mobility under magnetic field.

It is worthy mentioning that quantum materials can be generally categorized into three regimes according to the strength of electron-electron correlation, i.e. the weak-coupling regime with negligible correlation, the strong-coupling regime with large correlation, and the intermediate regime between these two limits. In contrast to the well-studied weak-coupling regime using the band-structure language and the strong-coupling regime as exemplified by high-*T*c cuprates, the intermediate regime is largely unexplored from both the theoretical and the experimental points of view [39]. To further explore this regime, Yang et al. performed an epitaxial strain study on the $[(SrIrO_3)1/(SrTiO_3)1]$ SL, aiming to modulate electron correlation in the effective 2D Hubbard model through the intermediate regime [38]. Experimentally, a series of $[(SrIrO_3)1/(SrTiO_3)1]$ SLs were prepared on different substrates to impose various compressive strain states. A systematic suppression of the insulating state with increasing compressive strain was observed, suggesting a gradual reduction of electron correlation. More interestingly, an emergent metallic state at high temperaturess was established in the mostly compressed SL. By probing the magnetic properties of the SLs, it is found that the insulating strength scales with the magnitude of AFM order parameter with an almost constant factor. This feature is reminiscent of a Slater insulator, where reduced translation symmetry due to AFM ordering opens up simultaneously a charge gap, and in turn, the charge gap melts at exactly the AFM ordering temperature. However, the SLs also have features of the strong-correlation for Mott limit, such as a robust insulating state above T_{N}.

The coexistence of the Slater and Mott features demonstrates that the SLs should be described in the regime of the Slater-Mott crossover regime. In this context, the emergence of the metallic phase is a strong evidence for the SL being across the Slater-Mott crossover regime to the weak-limit side, as shown in Fig. 2d. The primary driving force for the modulation of electron correlation was unveiled to be the enhanced hopping integral between planar oxygen and Ir ions due to the compressive strain. One should note that while previous models predict a similar correlation modulation with epitaxial strain [40–42], the important energetic behaviors at high temperatures were not captured, because the many-body physics was largely overlooked in the theoretical protocols.

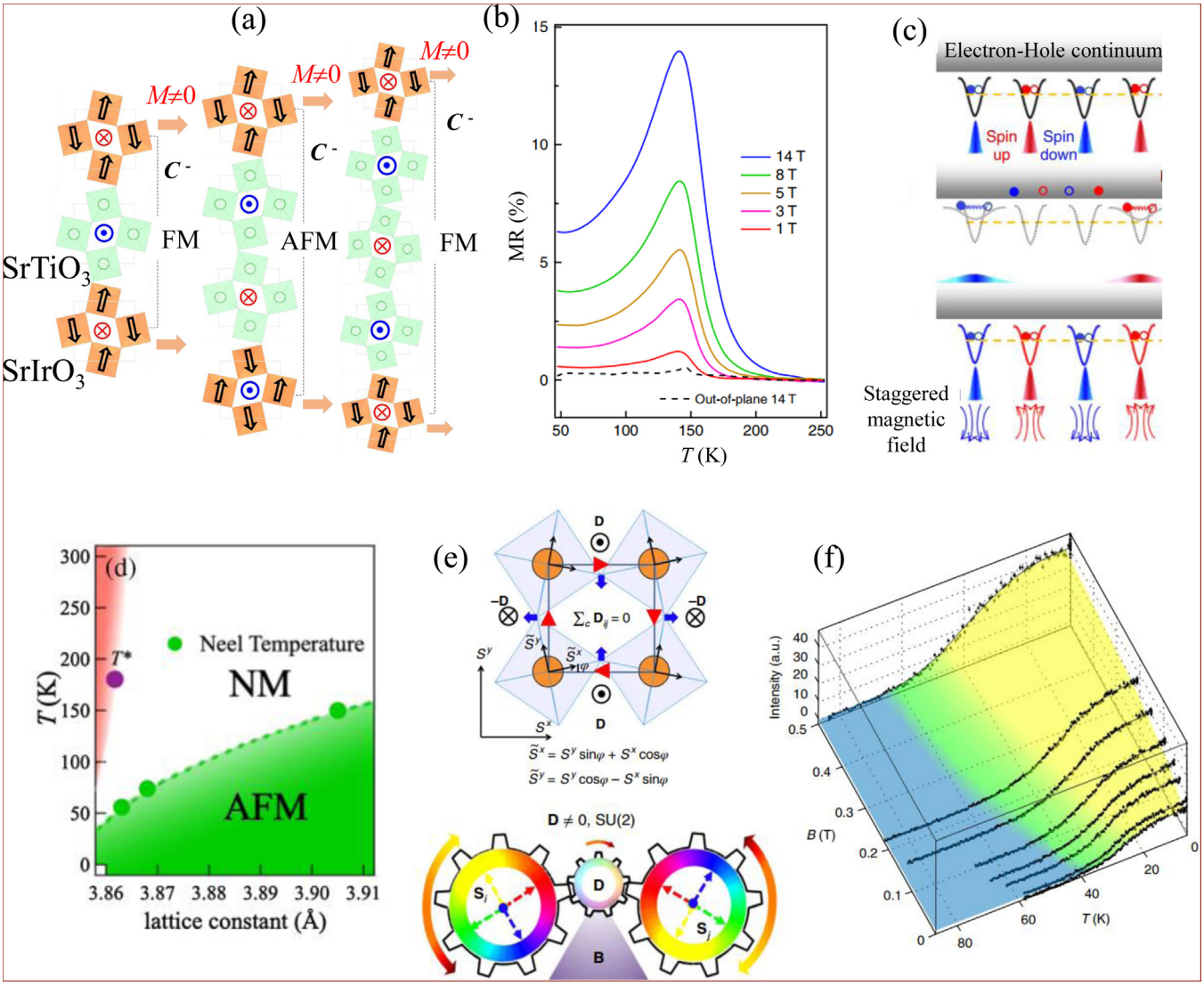

Fig. 2. Energetic charge and spin fluctuations in quasi-2D J_{eff} = 1/2 square lattice. (a) Modulation of magnetic interlayer coupling and octahedral rotation pattern in the [$(SrIrO_3)1/(SrTiO_3)m$] SLs (m = 1, 2, 3). Spin canting of the J_{eff} = 1/2 (black arrows) AFM ground state induces a net magnetic moment as illustrated with the orange arrows [34]. (b) Temperature-dependent MR under various magnetic fields for the [$(SrIrO_3)1/(SrTiO_3)1$] SL. (c) Schematic diagram from top to bottom, illustrating the AFM insulating ground state, the excited state with substantial longitudinal spin fluctuations and charge fluctuations, and the suppressed spin-charge fluctuations under the application of a staggered magnetic field. (d) Phase diagram of the compressively strained [$(SrIrO_3)1/(SrTiO_3)1$] SL. The green, white and red regions denote AFM-insulating, nonmagnetic (NM)-insulating and metallic- states, respectively. (e) Top panel is the staggered frame transformation of a rotation-only square lattice. Bottom panel is a cartoon illustrating the effect of the SU(2)-preserved DM interaction on the AFM order parameter. (d) Temperature-dependent magnetic scattering intensity under various fields of the [$(SrIrO_3)1/(SrTiO_3)2$] SL [37]. Panels (b) and (c) adapted from Ref. [36]. Panel (d) adapted from Ref. [38]. Panel (e) adapted from Ref. [37]. (For interpretation of the references to color in this figure legend, the reader is referred to the web version of this article.)

This difficulty is particularly serious in the intermediate regime, where multiple physical parameters are comparable in the energy scale, and a small variation of the parameters employed could lead to a dramatic difference during the calculations [39].

Under the strong correlation limit, the 2D Hubbard model can be projected on a 2D Heisenberg AFM model under the mean-field approximation. The [$(SrIrO_3)1/(SrTiO_3)2$] SLs thus represent an excellent material platform for studying the 2D quantum magnetism considering the strong correlation and the negligible interlayer coupling, as mentioned earlier. At first sight, a large Dzyaloshinskii–Moriya (DM) interaction and symmetric anisotropy interaction will break the spin isotropy. Nevertheless, it is shown that the two anisotropy terms can be gauged away simultaneously by a staggered frame transformation on the square lattice (Fig. 2e) [43]. The total Hamiltonian in the staggered local frame thus can be written as a single effective exchange term, which is isotropic, unveiling a so-called *hidden* SU(2) symmetry [10]. In other words, the pseudospin behaves essentially the same as a simple spin in the SL (i.e., while pseudospin-dependent hopping is not necessarily forbidden in a distorted lattice, it happens to be zero on the octahedral rotation-only square lattice). The [$(SrIrO_3)1/(SrTiO_3)2$] is thus expected to feature extreme spin fluctuations due to the 2D effective spin isotropy according to the Mermin-Wagner theorem [44].

An even more interesting situation arises when considering the Zeeman effect in the local staggered frame, which generates a large staggered field that allows one to drive the AFM order parameter with a uniform magnetic field. After applying an in-plane magnetic field to exploit the SU(2)-preserved DM interaction in the quasi-2D Heisenberg antiferromagnet, it was demonstrated that the extreme spin fluctuations can be significantly suppressed with a small magnetic field, giving rise to a drastic increase of the AFM ordering temperature, as shown in Fig. 2f.

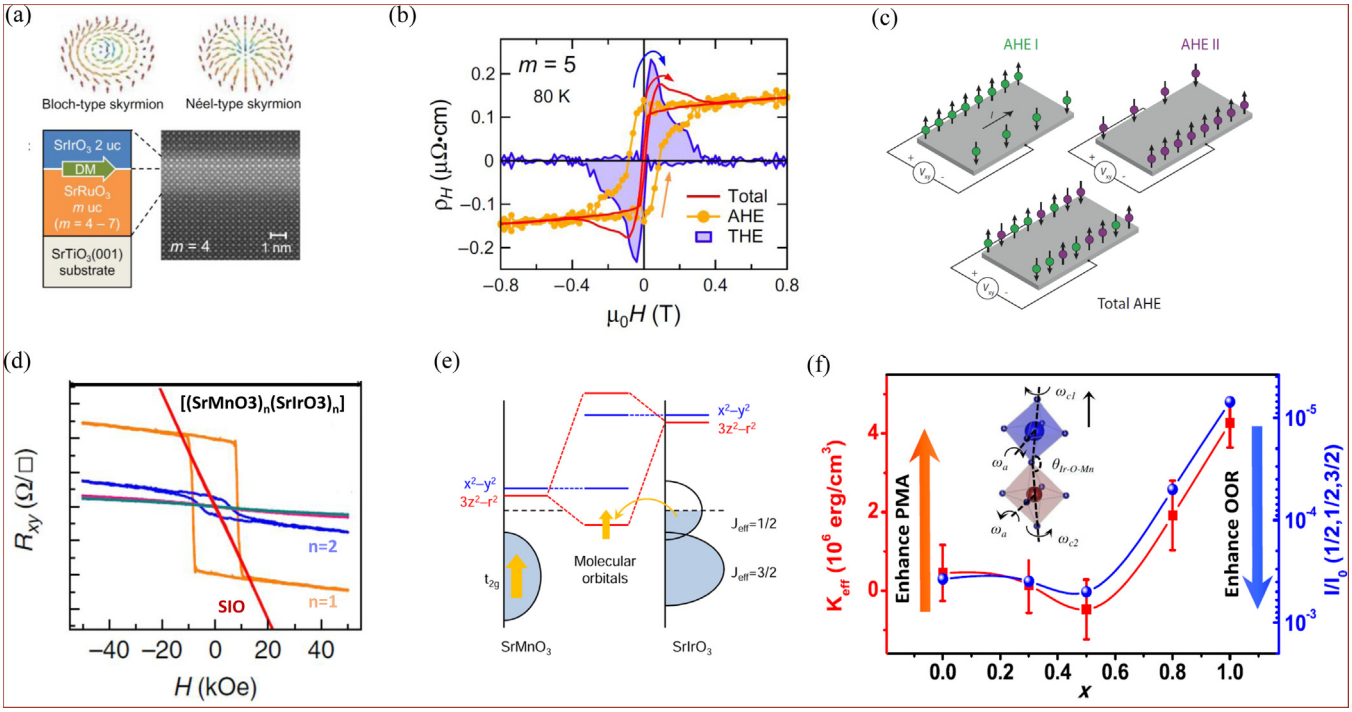

Fig. 3. Emergent magnetic phenomena in heterostructures of $SrIrO_3$ and 3*d*/4*d* oxides. (a) Schematics of Bloch and Néel type skyrmions in $SrRuO_3/SrIrO_3$ heterostructure. (b) Contribution of the Hall resistivity from AHE and THE. (c) Schematic diagram showing the contribution to the total AHE from two individual channels with different signs of AHE. (d) Hall resistances as a function of magnetic fields in $[(SrMnO_3)_n/(SrIrO_3)_n]$ SLs. (e) Schematic density of states of $SrMnO_3$ and $SrIrO_3$, and the consequent interfacial charge transfer between their molecular orbitals. (f) The correlation between PMA strength and oxygen octahedral rotations as revealed by half-order x-ray diffractions. Panels (a) and (b) adapted from Ref. [45]. Panel (c) adapted from Ref. [49]. Panel (d) adapted from Ref. [56]. Panel (e) adapted from Ref. [58]. Panel 3(f) adapted from Ref. [57].

This magnetic response is giant considering the fact that the magnetic field is more than three orders of magnitude smaller than the exchange coupling, while the ordering temperature was increased as large as 50%. Since this intriguing phenomenon allows for switching between a trivial disordered state and an AFM order state in temperatures well above T_N, it offers a new strategy to design AFM spintronics complementary to conventional routes, which define logic bits based on spin direction in the AFM ordering state. Nevertheless, future works such as enabling the electrical probe of the AFM switching, further optimizing the switching efficiency, and resolving the switching dynamics, chart the roadmap towards the applications.

4. Anomalous/Topological hall effects and magnetic anisotropy

Given the strong SOC in the 5*d* transition metal oxides, their interfaces with magnetic oxides provide vivid platforms to explore emergent magnetic phenomena and functionalities that could not be realized in the heterostructures comprised of either 3*d* or 4*d* complex oxides. Recent research endeavors have been mainly focused on two types of heterostructures, i.e., (i) the heterostructure of 5*d* $SrIrO_3$ and 4*d* $SrRuO_3$ [45–54] and (ii) the heterostructure of 5*d* $SrIrO_3$ and 3*d* $La_{1-x}Sr_xMnO_3$ [55–68].

Due to the intermediate electron correlation and SOC of 4*d* Ru cations, $SrRuO_3$ is an iterant ferromagnet with Curie temperature (T_c) around 160 K and large magneto-crystalline anisotropy energy [69]. The research interests in $SrRuO_3/SrIrO_3$ heterostructures were initially inspired by the discovery of the topological Hall effect (THE) by Matsuno et al. (Fig. 3a) [45]. As shown in Fig. 3b, the field-dependent Hall signals of the heterostructures consist of three contributions, i.e., the ordinary Hall effect that is linearly proportional to a magnetic field, the anomalous Hall effect (AHE) that is proportional to the magnetization, and THE that shows a characteristic hump feature. It is noted that THE has been previously observed in magnetic materials that host skyrmions or with noncoplanar spin structures [70,71]. Therefore, it was deduced that the observation of THE indicates the emergence of chiral magnetic textures in $SrRuO_3/SrIrO_3$ heterostructure, which is proposed to be stabilized by the interfacial DM interactions across the 4*d*/5*d* interfaces. Later on, Ohuchi et al. demonstrated that both AHE and THE of the $SrRuO_3/SrIrO_3$ heterostructures could be controlled by applying electric fields, which attracts further research attention due to the potential to manipulate chiral magnetic textures by an electric field [47].

Motivated by these discoveries, a great number of studies have been devoted to understanding the underlying mechanism of THE in $SrRuO_3/SrIrO_3$, which, however, revealed controversial conclusions. Firstly, it was found that heterostructures without $SrIrO_3$, such as $SrRuO_3$ films on $SrTiO_3$ or $BaTiO_3$, can also exhibit THE, which thereby raises doubts regarding the roles of 5*d* oxides with large SOC [72–74]. More importantly, the correlation between THE and chiral magnetic textures in the heterostructure remains elusive. Some results support the conclusion that THE is due to the chiral magnetic textures such as skyrmions (Fig. 3a) in ferromagnetic $SrRuO_3$, by studying the temperature-, field- and thickness- dependences of THE with various experimental methods, including magnetotransport and magnetic imaging [48,52,72,73]. By contrast, other studies imply that the “so-called” THE is probably due to the supposition of AHE signals from two conducting channels of $SrRuO_3$ that have different signs of AHE as well as different coercivity (Fig. 3c), which are likely arising from inhomogeneity of $SrRuO_3$ or the changes of Berry curvature by interfaces [49,51,53,74]. So far, this question is still under debate, and more direct evidence, such as atomic-scale imaging of magnetic textures are strongly demanded to fully resolve this issue. Nevertheless, the manipulation of Berry curvature of $SrRuO_3$ through heterointerfaces (e.g. $SrRuO_3/SrIrO_3$) and epitaxial strain has been established both theoretically and experimentally [49,53,74,75], which could be employed to engineer materials for magnetic applications.

Besides the observation of THE, the $SrRuO_3/SrIrO_3$ interfaces also exhibit other interesting phenomena, such as the spin-glass states and the tuning of perpendicular magnetic anisotropy energy [46,50]. Furthermore, Nelson et al. demonstrated that the metallic state is preserved down to one unit-cell of $SrIrO_3$ when interfacing with $SrRuO_3$ by using angle-resolved photoemission spectroscopy [54]. This is in stark contrast to the dimensionality-driven metal-insulator transition typically observed in complex oxides and signifies the critical roles of reconstruction of electronic states through the heterointerface.

The 3*d* manganite oxides, as exemplified by the chemical formula $La_{1-x}Sr_xMnO_3$, provide another family of magnetic oxides with rich electronic and magnetic properties depending on their stoichiometry and crystal structure [76]. Since the SOC is relatively weak in 3*d* Mn cations, the heterointerfaces with 5*d* oxides could potentially show emergent phenomena that are dramatically different from the parent constituents with the ingredient of SOC. Recent studies have revealed many interesting results in this material system.

Firstly, while $SrIrO_3$ is a paramagnetic metal in bulk, it was found to exhibit emergent magnetic ordering when interfacing with $La_{1-x}Sr_xMnO_3$. In SLs comprised of ferromagnetic $La_{0.7}Sr_{0.3}MnO_3$ and $SrIrO_3$, Yi et al. observed a clear XMCD signals at the x-ray absorption edges of Ir cations, revealing a net ferromagnetization in Ir antiparallel to that of the Mn counterpart [55]. Subsequent magnetic scattering measurement by Kim et al. revealed the emergent AFM ordering as deviation from ideal $J_{\text{eff}} = 1/2$ states in the ultrathin $SrIrO_3$ in the SLs [59]. It is noted that similar results have also been observed in SLs of $SrIrO_3$ and manganite with other stoichiometry, such as $LaMnO_3$ [65]. Therefore, these results demonstrate a universal approach that the magnetic ground states of 5*d* $SrIrO_3$ can be effectively manipulated by interfacial hybridization with other oxides.

Secondly, a clear charge transfer has been observed at the interfaces of $SrIrO_3$ and $La_{1-x}Sr_xMnO_3$, especially the manganite with empty e_g orbitals (e.g. $SrMnO_3$). Nichols et al. observed emergent ferromagnetism in the SLs comprised of AFM $SrMnO_3$ and $SrIrO_3$ (Fig. 3d) [56]. This effect is ascribed to the transfer of electrons from Ir to Mn cations at interfaces due to orbital hybridizations (Fig. 3e) [58]. Further studies also revealed that this interfacial charge transfer depends on many factors, such as the epitaxial strain [58], the stoichiometry [57], as well as the interfacial polar discontinuity [60]. Besides the emergent ferromagnetism, it is noted that the $[(SrMnO_3)1/(SrIrO_3)1]$ SLs also exhibit a strong perpendicular magnetic anisotropy (PMA) with an out-of-plane easy axis, leading to an emergent AHE signal with a large anomalous Hall conductivity (Fig. 3d). A recent study on $SrIrO_3/La_{1-x}Sr_xMnO_3$ bilayers by Yoo et al. revealed that the large AHE signals is likely arising from the proximity-induced magnetism in the $SrIrO_3$ with strong SOC [66].

Moreover, the observation of out-of-plane easy axis in the $[(SrMnO_3)1/(SrIrO_3)1]$ SLs implies that the strong PMA is induced by the interfacial coupling since both the shape anisotropy energy and magnetostrictive energy would otherwise favor easy-plane anisotropy. By carefully studying the $[(La_{1-x}Sr_xMnO_3)1/(SrIrO_3)1]$ SLs with different *x*, a correlation between PMA strength and oxygen octahedral rotations at interfaces has been established (Fig. 3f) [57]. Additionally, it has been shown that this interface-driven PMA strength could be further levitated by using epitaxial strains. As a result, heterostructures with strong PMA and high Curie temperature were realized by tuning the competition between bulk-like contribution and interfacial contribution to the magnetic anisotropy energy [67].

Given the tunable PMA strength, interfacial DM interactions and inversion symmetry breaking, chiral magnetic textures might also exist at the manganite-iridate interfaces, which has been theoretically demonstrated by using Monte Carlo technique [62]. The THE signals have been observed in bilayers and SLs of $SrIrO_3$ and $La_{1-x}Sr_xMnO_3$ [61,63]. In addition, Skoropata et al. found that the magnitudes of THE signals can be tuned by engineering the interfacial inversion symmetry at the atomic scale, suggesting that this effect is strongly correlated to the interfaces [63]. However, similar to the debates in $SrRuO_3/SrIrO_3$ heterostructures, the correlation between THE and chiral magnetic textures has yet to be demonstrated.

Besides the two model systems above, investigations on heterostructures of $SrIrO_3$ and other 3d complex oxides with partially filled *d* electrons have also emerged recently. Liu et al. studied the $LaNiO_3/SrIrO_3$ heterostructure and observed a significant interfacial charge transfer (about a full electron per cation at the interface), along with a significant structural and electronic reconstruction that leads to the breakdown of the SOC picture [77]. Jaiswal et al. studied the $LaCoO_3/SrIrO_3$ heterostructure and observed a pronounced AHE signal. Differing from metallic manganites or ruthenates, the insulating nature of ferromagnetic $LaCoO_3$ reveals the strong correlation between AHE signals and induced ferromagnetism (perhaps canted antiferromagnetism) in $SrIrO_3$ [78]. This conclusion is further verified in the heterostructure of $SrIrO_3$ and insulating AFM $LaFeO_3$ by the same research group [79]. It remains intriguing to explore the rich physics and potential functionalities in a wide range of 3*d*-5*d* and 4*d*-5*d* heterostructures.

5. Emergent electronic states induced by ionic control

The chemical substitution is a critical approach to manipulating the electronic states in complex oxides through electron filling, leading to the discovery of high-temperature superconductivity, colossal magnetoresistance, etc. However, this approach is hindered in 5*d* oxides due to their high melting temperatures, poor chemical solubility as well as strongly distorted octahedral complex. Over the last few years, the control of ionic evolution has developed rapidly as a promising pathway to manipulate the electronic states in complex oxides. In complementary to controlling atomic stacking through chemical substitution by growing materials at high temperatures, the ionic evolution approach modulates the chemical composition, lattice structure, and valance state at room temperature with soft-chemical approaches, demonstrating a unique opportunity to generate a series of metastable phases.

One of the effective pathways is the ionic liquid gating (ILG) method [80], which was developed several decades ago to achieve large electrostatic modulation, while an unintended electrochemical reaction is largely employed nowadays. As shown in Fig. 4a, under the application of an external electric field, small ions (for instance, H^+ and O^{2-}, stemming from the electrolyzed H_2O molecules) can be generated within the ionic liquid and intercalated into or de-intercalated from the oxide films [81–85]. Due to the principle of charge neutrality, the intercalation of every H^+ (or O^{2-}) ion leads to the injection of one electron (or two holes) into the transition metal *d* orbitals [86], hence dramatically altering the corresponding electronic states. Yi et al. exploited ILG on $La_{1-x}Sr_xMnO_3$ and $SrIrO_3$ single phase films, as well as $La_{1-x}Sr_xMnO_3/SrIrO_3$ SLs (Fig. 4b) [87]. They revealed that, compared with the single-phase materials, the SLs with ordered 3*d*-5*d* stacking favor the diffusivity of oxygen/hydrogen ions into the lattice, due to their tolerable octahedral distortion and cation-oxygen bonding. In stark contrast, both $La_{1-x}Sr_xMnO_3$ and $SrIrO_3$ are readily decomposed during the ILG with large voltage. Thus, the artificial SLs show great advantages as a platform to realize 5*d* band manipulation through ILG-induced ionic evolution.

Wang et al. carried out studies on the $[(SrIrO_3)1/(SrTiO_3)1]$ SL [88], which is considered as a spin-orbit Mott insulator, with the analogy to the Sr_2IrO_4, as shown in Figs. 4c and 4d [33,89]. Prior theoretical studies proposed that the 2D IrO_2-plane with appropriate electron doping could host a high-temperature superconducting state [20,21], which, however, is hindered by the instability of reduced Ir^{3+}, as well as low solid solubility in solid-state doped Sr_2IrO_4 [90,91]. As a matter of fact, a complete phase diagram as a function of electron doping for this system was still lacking. Ravichandran et al. exploited ILG technique on Sr_2IrO_4, which, however, only shows a minimal electron doping effect [92]. Wang et al. utilized the $[(SrIrO_3)1/(SrTiO_3)1]$ SL as the platform and demonstrated ILG-induced hydrogen intercalation

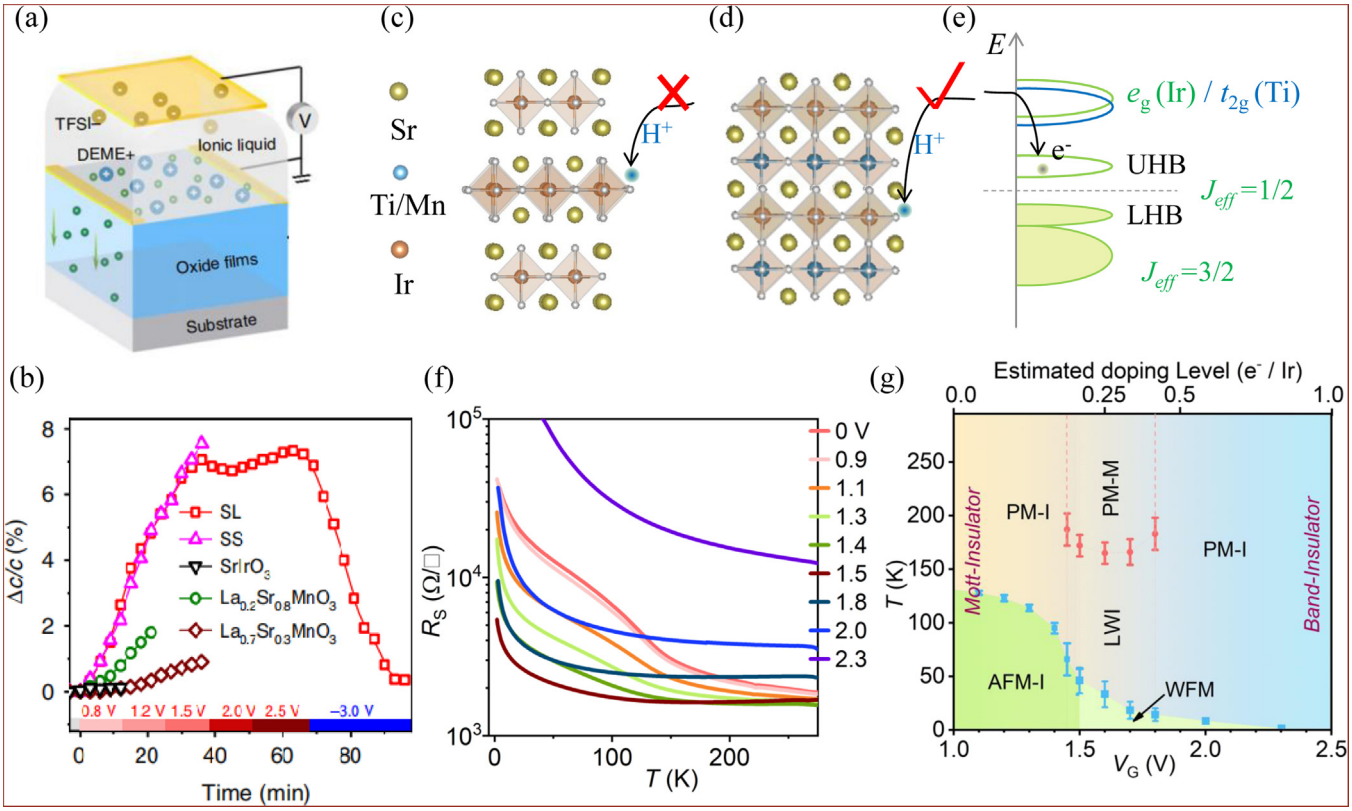

Fig. 4. Electrical-control of ionic evolution in iridate SLs. (a) Schematic of ILG method that induces the ionic transfer between oxide films and ionic liquid (DEME-TFSI). (b) Modulation of out-of-plane lattice constant (Δc/c) of a series of samples with the application of external voltage during ILG. SS refers to $Sr(Mn_{0.5}Ir_{0.5})O_3$ and SL refers a $La_{0.2}Sr_{0.8}MnO_3/SrIrO_3$ SL. The single-phase materials were damaged with increasing gating voltage, while the SL shows a reversible lattice evolution [87]. Lattice structures of Sr_2IrO_4 (c), and $[(SrIrO_3)1/(SrTiO_3)1]$ SL (d). (e) Schematic illustration of band alignment near Fermi level for the $[(SrIrO_3)1/(SrTiO_3)1]$ SL according to the Mott-Hubbard model. (f) Temperature-dependent resistance of $[(SrIrO_3)1/(SrTiO_3)1]$ SL during ILG. (g) Phase diagram of the hydrogenated $[(SrIrO_3)1/(SrTiO_3)1]$ SL as a function of gating voltage. PM-I, PM-M, LWI, WFM, and AFM-I refer to paramagnetic-insulator, paramagnetic-metal, localized weak insulator, weak ferromagnetism, and antiferromagnetic-insulator phases, respectively [88]. Panels (e) and (g) adapted from Ref. [88].

with continuous electron doping into the upper Hubbard band (UHB), as shown in Figs. 4d and 4e [88]. Fig. 4f shows the temperature dependence of resistance with variable gating voltage. The electron doping in the SL shows a rich phase diagram as shown in Fig. 4g. Explicitly, with increasing doping level, the parent Mott-insulator is first tuned into a localized metallic state with gradually suppressed magnetic ordering, then evolved into a nonmagnetic band insulating state with fully-occupied UHB. First-principles calculations indicate that the intercalated hydrogen ions prefer to form OH group with the equatorial oxygens of the IrO_2 planes. The intercalation in turn enhances lattice distortion and impurity scattering, which may account for the absence of a pure metallic state and a potential superconductivity [88]. Nevertheless, this work identifies that hydrogen doping could be a productive pathway for searching emergent electronic states in SLs, and replacing the $SrTiO_3$ with other band insulator to stabilize the SL lattice at higher symmetry (with released distortion) is a promising approach to pursue more intriguing electronic states.

Beyond the ILG-controlled H^+/O^{2-} evolution in 3*d*-5*d* SLs, it is important to note that Li^+ can also be employed as the shuttling ion to design new phases. Kuriyama et al. grew the spinel $Li_xIr_2O_4$ films and employed de-intercalation of Li ions to obtain a previously undiscovered λ-phase IrO_2 [93]. This new iridate shows a frustrated Ir-Ir tetrahedral geometry, which is identical to that in pyrochlore iridates, while the complicated/elusive *f*-electrons from rare-earth elements is eliminated [94]. In contrast to the metallic ground state observed in the rutile IrO_2 [95], the λ-phase IrO_2 shows a weak insulating behavior with a narrow Mott gap. Along this vein, the ion intercalation/de-intercalation represents an efficient route to tailor the crystal structure as well as electronic state of the iridate-based artificial structures, in order to obtain novel phases as well as exotic functionalities.

6. Outlook

As exemplified by this short review, there is no doubt that $SrIrO_3$-based artificial structures afford unprecedented pathways to achieve emergent phenomena for the 5*d* electron systems. However, a comprehensive understanding in the thermal dynamics of the epitaxial growth of iridates is still lacking. This renders the search for an optimal growth condition that is suitable for both iridate and other constituents in preparing high-quality iridate-based artificial heterostructures a grand challenge. Developing a robust epitaxial growth recipe for iridates is thus critical to prompt the research progress on iridate-based artificial structures and is necessary for synthesizing artificial structures using iridates with complex lattice structures such as the pyrochlore iridate. The latter leads to extra possibilities in exploiting emergent phenomena in the iridate-based artificial structures. For example, it was recently shown that SLs of $Sr_2IrO_4/SrTiO_3$ and $Sr_2IrO_4/BaTiO_3$ feature an emergent magnetoelectric phase transition with artificially designed ferroelectricity by virtue of an exotic interfacial DM interaction on the non-equivalent interface [96]. By stacking Sr_2IrO_4 and $Sr_3Ir_2O_7$ into a new superstructure, Kim et al. argued the realization of a model two-dimensional quantum Heisenberg antiferromagnet [97]. A robust growth recipe also underlies the experimental investigation of fascinating theoretical proposals based on sophisticated lattice design, with a profound example as the topological semimetal phase with helicoid surface states, predicted on a $[(SrIrO_3)2/(CaIrO_3)2]$ SL. The exotic

quantum Hall effect predicted in $SrIrO_3$-based SLs growing along the (111)-direction [98,99] is another attractive yet challenging candidate on the long list of theoretical proposals waiting for experimental investigation.

While the weak coupling limit studies render iridates an elegant candidate for exploring topological nontrivial states, it would be even more interesting to study how or to what extent the band topology would be altered by the electron correlation. In fact, iridates are believed to be a rare platform where electronic topology and electron correlation coexist and interact in an intriguing manner. Considering the controllability of both the spin-dependent hopping-governed electronic topology and spin-independent hopping-dominated effective electron correlation, as offered by artificial lattice design, iridate-based artificial structures may hold the key to resolving the elusive interplay between topology and correlation. A compelling route towards this end is to build toy-model materials to directly capture all these essential elements [100]. Profound questions, like, how nontrivial spin-dependent hopping affects the correlation-driven Hubbard band in square-lattice materials and how different topological nontrivial states would evolve under the electronic correlation, are expected to be answered by carefully designing crystal symmetry and chemical composition within the framework of iridate-based artificial structures. By utilizing advanced experimental protocols under extreme conditions such as ultra-low temperatures and ultra-high magnetic fields, one may gain additional insights from the emergent phenomena of artificial structures. For example, an anomalous MR was recently detected on a heterostructure composed of nonmagnetic conducting $Bi_2Ir_2O_7$ and insulating spin ice $Dy_2Ti_2O_7$ upon breaking the ice rule at sub-K temperatures [101]. Considering the fact that most frustrated magnets are insulating, the achieved electronic probe represents an essential step towards electronic device designing by utilizing exotic magnetic states of localized magnetic moments. Furthermore, utilization of electric-driven external stimuli, like proton-injection during ILG and in-situ strain/stress enabled with piezo-strain cells and freestanding membranes, on the iridate-based artificial structures is still in the early stage, which however would showcase the great application potential of these emergent phenomena.

Declaration of competing interest

The authors declare that they have no known competing financial interests or personal relationships that could have appeared to influence the work reported in this paper.

Acknowledgements

P. Y. acknowledges support from the NSFC under grant No. 51872155, the Beijing Nature Science Foundation (Z200007), and the Ministry of Science and Technology of China (Nos. 2021YFE0107900 and 2021YFA1400300). L. H. acknowledges support from the High Magnetic Field Laboratory of Anhui Province (AHHM-FX-2021–03) and the NSFC under Grant No. 12104460. D. Y. acknowledges support from the NSFC under Grant No. 92163113 and No. 52002204. J.L acknowledges support from the National Science Foundation under Grant No. DMR-1848269.

References

[1] W. Witczak-Krempa, G. Chen, Y.B. Kim, et al., Correlated quantum phenomena in the strong spin-orbit regime, Annu. Rev. Condens. Matter Phys. 5 (2014) 57–82.
[2] J.G. Rau, E.K.-H. Lee, H.-Y. Kee, Spin-Orbit physics giving rise to novel phases in correlated systems: iridates and related materials, Annu. Rev. Condens. Matter Phys. 7 (2016) 195–221.
[3] R. Schaffer, E.K.H. Lee, B.J. Yang, et al., Recent progress on correlated electron systems with strong spin-orbit coupling, Rep. Prog. Phys. 79 (2016) 094504.
[4] C. Martins, M. Aichhorn, S. Biermann, Coulomb correlations in 4d and 5d oxides from first principles—Or how spin–orbit materials choose their effective orbital degeneracies, J. Phys. 29 (2017) 263001.
[5] G. Cao, P. Schlottmann, The challenge of spin–orbit-tuned ground states in iridates: a key issues review, Rep. Prog. Phys. 81 (2018) 042502.
[6] J. Bertinshaw, Y.K. Kim, G. Khaliullin, et al., Square Lattice Iridates, Annu. Rev. Condens. Matter Phys. 10 (2019) 315–336.
[7] C. Lu, J.-M. Liu, The Jeff = 1/2 Antiferromagnet Sr2IrO4: a Golden avenue toward new physics and functions, Adv. Mater. 32 (2020) 1904508.
[8] S. Bhowal, I. Dasgupta, Spin–orbit effects in pentavalent iridates: models and materials, J. Phys. 33 (2021) 453001.
[9] Y. Okamoto, M. Nohara, H. Aruga-Katori, et al., Spin-Liquid state in the S=1/2 hyperkagome antiferromagnet Na4Ir3O8, Phys. Rev. Lett. 99 (2007) 137207.
[10] G. Jackeli, G. Khaliullin, Mott insulators in the strong spin-orbit coupling limit: from heisenberg to a quantum compass and kitaev models, Phys. Rev. Lett. 102 (2009) 017205.
[11] G. Khaliullin, W. Koshibae, S. Maekawa, Low energy electronic states and triplet pairing in layered cobaltate, Phys. Rev. Lett. 93 (2004) 176401.
[12] G. Khaliullin, Orbital order and fluctuations in mott insulators, Prog. Theor. Phys. Suppl. 160 (2005) 155–202.
[13] A. Shitade, H. Katsura, J. Kuneš, et al., Quantum spin hall effect in a transition metal oxide Na2IrO3, Phys. Rev. Lett. 102 (2009) 256403.
[14] F.D.M. Haldane, Model for a quantum hall effect without landau levels: condensed–matter realization of the "parity anomaly", Phys. Rev. Lett. 61 (1988) 2015–2018.
[15] B.-J. Yang, Y.B. Kim, Topological insulators and metal-insulator transition in the pyrochlore iridates, Phys. Rev. B 82 (2010) 085111.
[16] D. Pesin, L. Balents, Mott physics and band topology in materials with strong spin–orbit interaction, Nat. Phys. 6 (2010) 376.
[17] X. Wan, A.M. Turner, A. Vishwanath, et al., Topological semimetal and Fermi-arc surface states in the electronic structure of pyrochlore iridates, Phys. Rev. B 83 (2011) 205101.
[18] B.J. Kim, H. Jin, S.J. Moon, et al., Novel Jeff=1/2 Mott state induced by relativistic spin-orbit coupling in Sr2IrO4, Phys. Rev. Lett. 101 (2008) 076402.
[19] G. Cao, J. Bolivar, S. McCall, et al., *Weak ferromagnetism, metal-to-nonmetal transition, and negative differential resistivity in single-crystal* Sr_2IrO_4, Phys. Rev. B 57 (1998) R11039–R11042.
[20] F. Wang, T. Senthil, Twisted hubbard model for Sr2IrO4: magnetism and possible high temperature superconductivity, Phys. Rev. Lett. 106 (2011) 136402.
[21] H. Watanabe, T. Shirakawa, S. Yunoki, Monte Carlo study of an unconventional superconducting phase in iridium Oxide J = 1/2 mott insulators induced by carrier doping, Phys. Rev. Lett. 110 (2013) 027002.
[22] J.-M. Carter, V.V. Shankar, M.A. Zeb, et al., Semimetal and topological insulator in perovskite iridates, Phys. Rev. B 85 (2012) 115105.
[23] Y. Chen, Y.-M. Lu, H.-Y. Kee, Topological crystalline metal in orthorhombic perovskite iridates, Nat. Commun. 6 (2015) 6593.
[24] Y.F. Nie, P.D.C. King, C.H. Kim, et al., *Interplay of spin-orbit interactions, dimensionality, and octahedral rotations in semimetallic* $SrIrO_3$, Phys. Rev. Lett. 114 (2015) 016401.
[25] Z.T. Liu, M.Y. Li, Q.F. Li, et al., Direct observation of the Dirac nodes lifting in semimetallic perovskite SrIrO3 thin films, Sci. Rep. 6 (2016) 30309.
[26] T. Takayama, J. Chaloupka, A. Smerald, et al., Spin–orbit-entangled electronic phases in 4d and 5d transition-metal compounds, J. Phys. Soc. Jpn. 90 (2021) 062001.
[27] L. Hao, D. Meyers, M.P.M. Dean, et al., Novel spin-orbit coupling driven emergent states in iridate-based heterostructures, J. Phys. Chem. Solids 128 (2019) 39–53.
[28] D. Yi, N. Lu, X. Chen, et al., Engineering magnetism at functional oxides interfaces: manganites and beyond, J. Phys. 29 (2017) 443004.
[29] J. Chakhalian, X. Liu, G.A. Fiete, Strongly correlated and topological states in [111]grown transition metal oxide thin films and heterostructures, APL Mater. 8 (2020) 050904.
[30] A. Biswas, Y.H. Jeong, Growth and engineering of perovskite SrIrO3 thin films, Curr. Appl. Phys. 17 (2017) 605–614.
[31] L. Zhang, B. Pang, Y.B. Chen, et al., Review of spin–orbit coupled semimetal SrIrO3 in thin film form, Crit. Rev. Solid State Mater. Sci. 43 (2018) 367–391.
[32] B.J. Kim, H. Ohsumi, T. Komesu, et al., Phase-sensitive observation of a spin-orbital mott state in Sr2IrO4, Science 323 (2009) 1329–1332.
[33] J. Matsuno, K. Ihara, S. Yamamura, et al., Engineering a spin-orbital magnetic insulator by tailoring superlattices, Phys. Rev. Lett. 114 (2015) 247209.
[34] L. Hao, D. Meyers, C. Frederick, et al., Two-dimensional Jeff=1/2 antiferromagnetic insulator unraveled from interlayer exchange coupling in artificial perovskite iridate superlattices, Phys. Rev. Lett. 119 (2017) 027204.
[35] G. Cao, Y. Xin, C.S. Alexander, et al., Anomalous magnetic and transport behavior in the magnetic insulator Sr3Ir2O7, Phys. Rev. B 66 (2002) 214412.
[36] L. Hao, Z. Wang, J. Yang, et al., Anomalous magneto-resistance due to longitudinal spin fluctuations in a Jeff = 1/2 Mott semiconductor, Nat. Commun. 10 (2019) 5301.
[37] L. Hao, D. Meyers, H. Suwa, et al., Giant magnetic response of a two-dimensional antiferromagnet, Nat. Phys. 14 (2018) 806–810.
[38] J. Yang, L. Hao, D. Meyers, et al., Strain-modulated slater-mott crossover of pseudospin-half square-lattice in (SrIrO3)1/(SrTiO3)1 superlattices, Phys. Rev. Lett. 124 (2020) 177601.
[39] J.P.F. LeBlanc, A.E. Antipov, F. Becca, et al., Solutions of the two-dimensional hubbard model: benchmarks and results from a wide range of numerical algorithms, Phys. Rev. X 5 (2015) 041041.
[40] K.H. Kim, H.S. Kim, M.J. Han, Electronic structure and magnetic properties of iridate superlattice SrIrO3/SrTiO3, J. Phys. 26 (2014) 185501.
[41] S.Y. Kim, C.H. Kim, L.J. Sandilands, et al., Manipulation of electronic structure via alteration of local orbital environment in [(SrIrO3)m, (SrTiO3)](m=1, 2, and ∞) superlattices, Phys. Rev. B 94 (2016) 245113.
[42] B. Kim, P. Liu, C. Franchini, Dimensionality-strain phase diagram of strontium iridates, Phys. Rev. B 95 (2017) 115111.

[43] L. Shekhtman, O. Entin-Wohlman, A. Aharony, Moriya's anisotropic superexchange interaction, frustration, and Dzyaloshinsky's weak ferromagnetism, Phys. Rev. Lett. 69 (1992) 836–839.
[44] N.D. Mermin, H. Wagner, Absence of ferromagnetism or antiferromagnetism in one- or two-dimensional isotropic Heisenberg models, Phys. Rev. Lett. 17 (1966) 1133–1136.
[45] J. Matsuno, N. Ogawa, K. Yasuda, et al., Interface-driven topological Hall effect in SrRuO3-SrIrO3 bilayer, Sci. Adv. 2 (2016) e1600304.
[46] B. Pang, L.Y. Zhang, Y.B. Chen, et al., Spin-glass-like behavior and topological hall effect in SrRuO3/SrlrO3 superlattices for oxide spintronics applications, ACS Appl. Mater. Interfaces 9 (2017) 3201–3207.
[47] Y. Ohuchi, J. Matsuno, N. Ogawa, et al., Electric-field control of anomalous and topological Hall effects in oxide bilayer thin films, Nat. Commun. 9 (2018) 213.
[48] K.-Y. Meng, A.S. Ahmed, M. Baćani, et al., Observation of nanoscale skyrmions in SrIrO3/SrRuO3 bilayers, Nano Lett. 19 (2019) 3169–3175.
[49] D.J. Groenendijk, C. Autieri, T.C. van Thiel, et al., Berry phase engineering at oxide interfaces, Phys. Rev. Res. 2 (2020).
[50] Z. Zeng, J. Feng, X. Zheng, et al., Emergent ferromagnetism with tunable perpendicular magnetic anisotropy in short-periodic SrIrO3/SrRuO3 superlattices, Appl. Phys. Lett. 116 (2020) 142401.
[51] L. Wysocki, L. Yang, F. Gunkel, et al., Validity of magnetotransport detection of skyrmions in epitaxial SrRuO3 heterostructures, Phys. Rev. Mater. 4 (2020) 054402.
[52] S. Esser, J. Wu, S. Esser, et al., Angular dependence of Hall effect and magneto-resistance in SrRuO3-SrIrO3 heterostructures, Phys. Rev. B 103 (2021) 214430.
[53] D. Zheng, Y.-W. Fang, S. Zhang, et al., Berry phase engineering in SrRuO3/SrIrO3/SrTiO3 superlattices induced by band structure reconstruction, ACS Nano 15 (2021) 5086–5095.
[54] J.N. Nelson, N.J. Schreiber, A.B. Georgescu, et al., Interfacial charge transfer and persistent metallicity of ultrathin SrIrO3/SrRuO3 heterostructures, Sci. Adv. 8 (2022) eabj0481.
[55] D. Yi, J. Liu, S.L. Hsu, et al., Atomic-scale control of magnetic anisotropy via novel spin-orbit coupling effect in La2/3Sr1/3MnO3/SrIrO3 superlattices, PNAS 113 (2016) 6397–6402.
[56] J. Nichols, X. Gao, S. Lee, et al., Emerging magnetism and anomalous Hall effect in iridate–manganite heterostructures, Nat. Commun. 7 (2016) 12721.
[57] D. Yi, C.L. Flint, P.P. Balakrishnan, et al., Tuning perpendicular magnetic anisotropy by oxygen octahedral rotations in (La1-xSrxMnO3)/(SrIrO3) superlattices, Phys. Rev. Lett. 119 (2017) 077201.
[58] S. Okamoto, J. Nichols, C. Sohn, et al., Charge transfer in iridate-manganite superlattices, Nano Lett. 17 (2017) 2126–2130.
[59] J.W. Kim, Y. Choi, S.H. Chun, et al., Controlling entangled spin-orbit coupling of 5d states with interfacial heterostructure engineering, Phys. Rev. B 97 (2018).
[60] T. Yu, B. Deng, L. Zhou, et al., Polarity and spin-orbit coupling induced strong interfacial exchange coupling: an asymmetric charge transfer in iridate-manganite heterostructure, ACS Appl. Mater. Interfaces 11 (2019) 44837–44843.
[61] Y. Li, L.Y. Zhang, Q.H. Zhang, et al., Emergent topological hall effect in La0.7Sr0.3MnO3/SrIrO3 heterostructures, ACS Appl. Mater. Interfaces 11 (2019) 21268–21274.
[62] N. Mohanta, E. Dagotto, S. Okamoto, Topological Hall effect and emergent skyrmion crystal at manganite-iridate oxide interfaces, Phys. Rev. B 100 (2019) 064429.
[63] E. Skoropata, J. Nichols, J.M. Ok, et al., Interfacial tuning of chiral magnetic interactions for large topological Hall effects in LaMnO3/SrIrO3 heterostructures, Sci. Adv. 6 (2020) eaaz3902.
[64] T.S. Suraj, G.J. Omar, H. Jani, et al., Tunable and enhanced Rashba spin-orbit coupling in iridate-manganite heterostructures, Phys. Rev. B 102 (2020) 125145.
[65] Y. Zhang, Y.Z. Luo, L. Wu, et al., Interfacial-hybridization-modified Ir ferromagnetism and electronic structure in LaMnO3/SrIrO3 superlattices, Phys. Rev. Res. 2 (2020) 033496.
[66] M.-W. Yoo, J. Tornos, A. Sander, et al., Large intrinsic anomalous Hall effect in SrIrO3 induced by magnetic proximity effect, Nat. Commun. 12 (2021) 3283.
[67] D. Yi, H. Amari, P.P. Balakrishnan, et al., Enhanced interface-driven perpendicular magnetic anisotropy by symmetry control in oxide superlattices, Phys. Rev. Appl. 15 (2021).
[68] Z. Ren, B. Lao, X. Zheng, et al., Emergence of insulating ferrimagnetism and perpendicular magnetic anisotropy in 3d-5d perovskite oxide composite films for insulator spintronics, ACS Appl. Mater. Interfaces 14 (2022) 15407–15414.
[69] G. Koster, L. Klein, W. Siemons, et al., Structure, physical properties, and applications of SrRuO3 thin films, Rev. Mod. Phys. 84 (2012) 253–298.
[70] Y. Taguchi, Y. Oohara, H. Yoshizawa, et al., Spin chirality, berry phase, and anomalous hall effect in a frustrated ferromagnet, Science 291 (2001) 2573–2576.
[71] Y. Tokura, M. Kawasaki, N. Nagaosa, Emergent functions of quantum materials, Nat. Phys. 13 (2017) 1056–1068.
[72] L.F. Wang, Q.Y. Feng, Y. Kim, et al., Ferroelectrically tunable magnetic skyrmions in ultrathin oxide heterostructures, Nat. Mater. 17 (2018) 1087.
[73] Q. Qin, L. Liu, W. Lin, et al., Emergence of topological hall effect in a SrRuO3 single layer, Adv. Mater. 31 (2019) 1807008.
[74] L. Wu, F.D. Wen, Y.X. Fu, et al., Berry phase manipulation in ultrathin SrRuO3 films, Phys. Rev. B 102 (2020).
[75] D. Tian, Z. Liu, S. Shen, et al., Manipulating Berry curvature of SrRuO3 thin films via epitaxial strain, PNAS 118 (2021) e2101946118.
[76] Y. Tokura, Critical features of colossal magnetoresistive manganites, Rep. Prog. Phys. 69 (2006) 797–851.
[77] X.R. Liu, M. Kotiuga, H.S. Kim, et al., Interfacial charge-transfer Mott state in iridate-nickelate superlattices, PNAS 116 (2019) 19863–19868.
[78] A.K. Jaiswal, D. Wang, V. Wollersen, et al., Direct observation of strong anomalous hall effect and proximity-induced ferromagnetic state in SrIrO3, Adv. Mater. 34 (2022) 2109163.
[79] A.K. Jaiswal, R. Schneider, M.L. Tacon, et al., Magnetotransport of SrIrO3-based heterostructures, AIP Adv. 12 (2022) 035120.
[80] S.Z. Bisri, S. Shimizu, M. Nakano, et al., Endeavor of iontronics: from fundamentals to applications of ion-controlled electronics, Adv. Mater. 29 (2017) 1607054.
[81] N. Lu, P. Zhang, Q. Zhang, et al., Electric-field control of tri-state phase transformation with a selective dual-ion switch, Nature 546 (2017) 124.
[82] Y. Cui, G. Zhang, H. Li, et al., Protonation induced high-Tc phases in iron-based superconductors evidenced by NMR and magnetization measurements, Sci. Bull. 63 (2018) 11–16.
[83] M. Wang, X. Sui, Y. Wang, et al., Manipulate the electronic and magnetic states in NiCo2O4 films through electric-field-induced protonation at elevated temperature, Adv. Mater. 31 (2019) e1900458.
[84] Z. Li, S. Shen, Z. Tian, et al., Reversible manipulation of the magnetic state in SrRuO3 through electric-field controlled proton evolution, Nat. Commun. 11 (2020) 184.
[85] Q. Lu, S. Huberman, H. Zhang, et al., Bi-directional tuning of thermal transport in SrCoOx with electrochemically induced phase transitions, Nat. Mater. 19 (2020) 655–662.
[86] T. Katase, T. Onozato, M. Hirono, et al., A transparent electrochromic metal-insulator switching device with three-terminal transistor geometry, Sci. Rep. 6 (2016) 25819.
[87] D. Yi, Y. Wang, O.M.J. van 't Erve, et al., Emergent electric field control of phase transformation in oxide superlattices, Nat. Commun. 11 (2020) 902.
[88] M. Wang, L. Hao, F. Yin, et al., Manipulate the electronic state of mott iridate superlattice through protonation induced electron-filling, Adv. Funct. Mater. 2021 (2021) 2100261.
[89] S.J. Moon, H. Jin, K.W. Kim, et al., Dimensionality-controlled insulator-metal transition and correlated metallic state in 5d transition metal oxides Srn+1IrnO3n+1 (n=1, 2, and ∞), Phys. Rev. Lett. 101 (2008) 226402.
[90] M. Ito, M. Uchida, Y. Kozuka, et al., Effective carrier doping and metallization in LaxSr2−x−yBayIrO4−δ thin films, Phys. Rev. B 93 (2016) 045139.
[91] Y.J. Yan, M.Q. Ren, H.C. Xu, et al., Electron-doped Sr2IrO4: an analogue of hole–doped cuprate superconductors demonstrated by scanning tunneling microscopy, Phys. Rev. X 5 (2015) 041018.
[92] J. Ravichandran, C.R. Serrao, D.K. Efetov, et al., Ambipolar transport and magneto-resistance crossover in a Mott insulator Sr2IrO4, J. Phys. 28 (2016) 505304.
[93] H. Kuriyama, J. Matsuno, S. Niitaka, et al., Epitaxially stabilized iridium spinel oxide without cations in the tetrahedral site, Appl. Phys. Lett. 96 (2010).
[94] K. Ueda, J. Fujioka, B.J. Yang, et al., Magnetic field-induced insulator-semimetal transition in a pyrochlore Nd2Ir2O7, Phys. Rev. Lett. 115 (2015) 056402.
[95] M. Uchida, W. Sano, K.S. Takahashi, et al., Field-direction control of the type of charge carriers in nonsymmorphic IrO2, Phys. Rev. B 91 (2015).
[96] X. Liu, W. Song, M. Wu, et al., Magnetoelectric phase transition driven by interfacial-engineered Dzyaloshinskii-Moriya interaction, Nat. Commun. 12 (2021) 5453.
[97] H. Kim, J. Bertinshaw, J. Porras, et al., $Sr_2IrO_4/Sr_3Ir_2O_7$ *superlattice for a model two-dimensional quantum Heisenberg antiferromagnet*, Phys. Rev. Res. 4 (2022) 013229.
[98] F. Wang, Y. Ran, Nearly flat band with Chern number C=2 on the dice lattice, Phys. Rev. B 84 (2011) 241103.
[99] D. Xiao, W. Zhu, Y. Ran, et al., Interface engineering of quantum Hall effects in digital transition metal oxide heterostructures, Nat. Commun. 2 (2011) 596.
[100] J. Yang, H. Suwa, D. Meyers, et al., Quasi-two-dimensional anomalous hall mott insulator of topologically engineered Jeff=1/2 electrons, Phys. Rev. X 12 (2022) 031015.
[101] H. Zhang, K. Noordhoek, C.K. Xing, et al., *Anomalous magneto-resistance by breaking ice rule in Bi2Ir2O7/Dy2Ti2O7 heterostructure*, arXiv:2011.09048 (2020).

Lin Hao is an experimental scientist in the High magnetic field Lab, Hefei institutes of Physical Science, Chinese Academy of Sciences. After receiving his Ph.D. from The University of Science and Technology of China in 2016, he moved to University of Tennessee to work as a postdoc till 2020. He joined the High magnetic field lab as an independent PI in the end of 2020, and his group focuses on the designing, synthesizing, and exploring emergent phenomena in iridate-based artificial structures.

Pu Yu is a professor at Department of Physics, Tsinghua University. He received his Ph.D. degree in Physics from University of California at Berkeley in 2011. After one-year postdoc stay at RIKEN Japan, he joined the faculty of Tsinghua University as an assistant professor in 2012, and was promoted to associate professor in 2017 and professor in 2018. His current research interest lies in understanding and designing novel electronic states of complex oxides.